



POLITECNICO
MILANO 1863

RE.PUBLIC@POLIMI

Research Publications at Politecnico di Milano

Post-Print

This is the accepted version of:

G. Gozzini, D. Invernizzi, S. Panza, M. Giurato, M. Lovera
Air-To-air Automatic Landing of Unmanned Aerial Vehicles: a Quasi Time-Optimal Hybrid Strategy
IEEE Control Systems Letters, Vol. 4, N. 3, 2020, p. 692-697
doi:10.1109/LCSYS.2020.2991701

The final publication is available at <https://doi.org/10.1109/LCSYS.2020.2991701>

Access to the published version may require subscription.

When citing this work, cite the original published paper.

© 2020 IEEE. Personal use of this material is permitted. Permission from IEEE must be obtained for all other uses, in any current or future media, including reprinting/republishing this material for advertising or promotional purposes, creating new collective works, for resale or redistribution to servers or lists, or reuse of any copyrighted component of this work in other works.

Permanent link to this version

<http://hdl.handle.net/11311/1136901>

Air-to-Air Automatic Landing of Unmanned Aerial Vehicles: a quasi time-optimal hybrid strategy

Giovanni Gozzini¹, Davide Invernizzi¹, Simone Panza¹, Mattia Giurato¹, Marco Lovera¹

Abstract—It is well known that small electric Unmanned Aerial Vehicles (UAVs) suffer from low endurance problems. A possibility to extend the range of UAV missions could be to have a carrier drone with several lightweight multirotors aboard, which can take-off from and land on it. In this paper the challenging problem of Air-to-Air Automatic Landing (AAAL) of UAVs is solved by developing a strategy that combines a quasi-time optimal feedback and a hybrid logic to ensure a safe and fast landing. Eventually, the proposed algorithm is validated through experimental activities involving the landing of a small quadcopter on a bigger octocopter used as a carrier.

Index Terms—UAVs, Automatic landing, Hybrid control

I. INTRODUCTION

IN recent years, the study of Unmanned Aerial Vehicles (UAVs) has received increasing attention thanks to their wide range of application. When surveillance, reconnaissance and search-and-rescue missions are considered, small-scale UAVs are known to suffer from low endurance, being usually powered by batteries. To extend mission endurance, a possible solution is to use a carrier drone with smaller UAVs (followers) that can take-off from and land on it.

The problem of interaction among UAVs has been addressed in the context of formation flight control (see, *e.g.*, [1], [2]) and of Air-to-Air Automatic Refuelling (AAAR) (see, *e.g.*, [3]). Another challenging and technologically complex application involves the landing of Vertical Take Off and landing (VTOL) UAVs on the Landing Helicopter Dock (LHD) of a moving ship. There are also examples of landing of VTOL UAVs on a vertically oscillating platform [4] or on moving platforms [5], [6], [7], although none of them involves a flying platform.

In this paper the design of a procedure enabling Air-to-Air Automatic Landing (AAAL) of UAVs in a non-collaborative scenario is investigated. This problem is not only technologically complex but it is also risky and dangerous. In the case of a multirotor, the wake of the propellers generates an unsteady flow field around it, such that, when flying close, the two UAVs perturb each other. While in previous works [8], [9] the air-to-air landing problem was addressed for the case of a hovering or slowly-moving target, in this paper we tackle the more challenging problem of landing on a moving target whose motion cannot be controlled but only measured. To this aim, we propose a landing strategy which combines a Quasi Time-Optimal (QTO) control law for tracking and a

hybrid logic to perform the landing in a safe manner. The problem is decomposed by referring to three operating modes: synchronization, approach and landing. By properly designing the switch conditions among the different modes, we show that the AAAL can be performed safely from a large domain of initial conditions. An experimental campaign has been carried out to verify the proposed landing procedure by using two multirotors which have been developed for this specific task [10]. In particular, a loiter condition for the carrier drone has been replicated by making it move along a circular trajectory.

II. AIR-TO-AIR LANDING: PROBLEM STATEMENT

In this section we introduce and formalize the problem of AAAL in which a follower UAV has to land over a larger UAV, called the target. While we will specifically refer to multirotor platforms for the experimental validation, the formulation is kept general by casting the landing problem as a kinematic stability problem, under suitable assumptions. Of course, obvious considerations regarding the size and weights of the two UAVs must be taken into account, *i.e.*, it is necessary that the carrier drone must be larger and heavier than the follower, in order to be able to stand its weight after touch-down. In the considered scenario, the follower has to perform the landing maneuver autonomously using only some information about the state of the target, whose motion cannot be controlled.

First of all, let us recall the dynamical model of the follower, considered as rigid UAV, which is described by

$$\dot{x}_f = v_f \quad (1)$$

$$m\dot{v}_f = -mge_3 + R_f(f_c + f_e), \quad (2)$$

$$\dot{R}_f = R_f S(\omega_f) \quad (3)$$

$$J\dot{\omega}_f = -S(\omega_f)J\omega_f + \tau_c + \tau_e \quad (4)$$

where $m \in \mathbb{R}_{>0}$ and $J = J^\top \in \mathbb{R}_{>0}^{3 \times 3}$ are, respectively, the mass and the inertia matrix of the follower, $g = 9.81 \text{ m/s}^2$ is the gravitational acceleration and $e_3 := [0 \ 0 \ 1]^\top$. Herein, the state of the follower has been identified with the tuple $(x_f, R_f, v_f, \omega_f)$, where $x_f \in \mathbb{R}^3$ is the position of the center of mass with respect to an inertial frame F_I , $R_f \in \text{SO}(3)$ is the rotation matrix describing the attitude of a body-fixed frame F_B with respect to F_I , while $v_f \in \mathbb{R}^3$ and $\omega \in \mathbb{R}^3$ are the translational and angular velocity, resolved in F_I and F_B , respectively. Finally, $(f_c, \tau_c), (f_e, \tau_e) \in \mathbb{R}^6$ are the control and disturbance wrench, respectively, both resolved in F_B while $S(\omega_f) = -S(\omega_f)^\top \in \mathbb{R}^{3 \times 3}$ is the skew-symmetric matrix associated with ω_f and such that $S(\omega_f)y = \omega_f \times y$ for any $y \in \mathbb{R}^3$.

¹G. Gozzini, D. Invernizzi, S. Panza, M. Giurato and M. Lovera are with Dipartimento di Scienze e Tecnologie Aerospaziali, Politecnico di Milano, Via La Masa 34, 20156 Milano, Italy {giovanni.gozzini, davide.invernizzi, simone.panza, mattia.giurato, marco.lovera}@polimi.it

In the following, it is assumed that there exist control laws for f_c and τ_c such that any bounded velocity trajectory $v_d(t)$ is asymptotically tracked¹. In this way we will be able to formulate the landing problem regardless of the specific UAV actuation mechanism by referring to the kinematic model

$$\dot{x}_f = u, \quad (5)$$

where $u \in \mathbb{R}^3$ is a virtual input, corresponding to the follower velocity in the inertial frame, to be used for control design².

Moreover, we will also assume basic requirements about the motion of the target as well as the availability of some information about its state.

Assumption 1: Smoothness and boundedness of the target trajectory. The trajectory of the target UAV $t \mapsto [x_t(t)^\top v_t(t)^\top]^\top \in \mathbb{R}^6$ satisfies $\dot{x}_t(t) = v_t(t)$, where $v_t \in \mathbb{R}^3$, velocity of the target measured in the inertial frame F_t , is assumed to be uniformly bounded and continuous.

Assumption 2: Knowledge of the follower and target states. The state of the follower (x_f, v_f) and the state of the target (x_t, v_t) are available for feedback at all times.

While the state of the follower is usually available onboard from a suitable state filter, the state of the target can be reconstructed onboard the follower by using a dedicated vision-based relative navigation system and or it can be provided by the target itself if communication between the two drones is possible.

The target should not be considered as a single point x_t but rather as a flat surface on which the follower can land:

$$\Omega_t(t) := \left\{ y \in \mathbb{R}^3 : e_3^\top (y - x_t(t)) = 0, \|y - x_t(t)\| \leq r_t \right\} \quad (6)$$

where $r_t \in \mathbb{R}_{>0}$, i.e., the target is identified with a flat surface moving with level attitude.

Remark 1: While we implicitly assume that the attitude of the target is constantly aligned with e_3 , generalizations of the landing problem to account for an arbitrary attitude motion are possible under the assumption that the target attitude is available to the landing algorithm. At the same time, we will propose a landing strategy robust to sufficiently small attitude motions of the target. \square

Problem 1: Consider the UAV kinematic model in equation (5), under Assumption 1 and 2, find a control law for u such that x_f converges *safely* to a point in the set Ω_t defined in (6) in finite time.

The adverb "safely" in Problem 1 encodes the requirement that the follower has to land from above the target and in a sufficiently slow manner, which will allow minimizing perturbation effects between each other. Indeed, a too fast approach would require a strong braking action on the part of the follower when close to the target: since the braking is achieved by increasing the rotor speed, the power of the wake impacting on the target propellers increases as well.

¹There exist several control design methods in the multirotor UAV literature which are suitable or can be easily adapted to this task see, e.g., [11], [12], [13], [14]. In our experiments we will make use of the controller already available in the PX4 autopilot [15], which can be customized to fit our design.

²Robustness against unmodeled dynamics will be addressed with a careful design of the hybrid logic in Section III-B (Remark 3).

III. AUTOMATIC LANDING STRATEGY

This section is devoted to presenting our landing strategy which combines a quasi time-optimal control law for tracking and a hybrid logic to perform the landing in a safe manner, as required by Problem 1.

A. Quasi time-optimal tracking

Under the assumption that the velocity of the follower UAV is directly controllable as in (5), we can use input u in a feedback strategy to track any sufficiently smooth trajectory, denoted here as $t \mapsto x_d(t) \in \mathbb{R}^3$. To this aim, let us introduce the tracking error

$$p := x_f - x_d \quad (7)$$

which we split in a planar and vertical component, defined respectively as $p_\perp := [p_1 \ p_2]^\top$ and p_3 . The corresponding error dynamics is given by

$$\dot{p} = u - \dot{x}_d = u - v_d. \quad (8)$$

where $v_d := \dot{x}_d$ is the desired velocity. By partitioning as well the input $u := [u_\perp^\top \ u_3]^\top = [u_1 \ u_2 \ u_3]^\top$, we propose the following control law

$$u_\perp(p_\perp, v_{d_\perp}) := -\text{sat}_{v_M}^\perp(p_\perp) + v_{d_\perp} \quad (9)$$

$$u_3(p_3, v_{d_3}) := -\text{sat}_{v_M}^{v_M}(k_3 p_3) + v_{d_3} \quad (10)$$

where $\text{sat}_{v_M}^{v_M}(p_3) := \min(\max(p_3, -v_M), v_M)$ is a scalar saturation function with saturation levels $v_m, v_M \in \mathbb{R}_{>0}$,

$$\text{sat}_{v_M}^\perp(p_\perp) := \min\left(k_\perp, \frac{v_M}{\|p_\perp\|}\right) p_\perp \quad (11)$$

and k_\perp, k_3 are scalar positive gains.

The control law has been split in a planar (9) and vertical (10) component for reasons that will become clear when presenting the hybrid logic. Note, in passing, that the specific selection in (11) with a scalar gain k_\perp makes the system axial-symmetric with respect to e_3 and allows us to study the behavior of closed-loop solutions in the cartesian plane identified by the axes $\|p_\perp\|$ and p_3 (See Figure 1).

The following theorem establishes the tracking properties of the proposed law.

Theorem 1: Consider system (5) controlled by (9)-(10). Given any desired trajectory $t \mapsto [x_d(t)^\top v_d(t)^\top]^\top \in \mathbb{R}^6$ such that $\dot{x}_d(t) = v_d(t)$, for any positive selection of gains k_\perp, k_3 and saturation levels v_m, v_M , the equilibrium point $p = 0$ is Globally Asymptotically Stable (GAS).

Proof 1: Consider the radially unbounded Lyapunov function $V_{p_\perp} := \frac{1}{2}\|p_\perp\|^2$: its time derivative along the flows of (8) controlled by (9) is $\dot{V}_{p_\perp} = p_\perp^\top (u_\perp - v_{d_\perp}) = -p_\perp^\top \text{sat}_{v_M}^\perp(p_\perp) = -\min(k_\perp \|p_\perp\|, v_M \|p_\perp\|) < 0 \ \forall p_\perp \neq 0$. By standard Lyapunov arguments, $p_\perp = 0$ is a GAS equilibrium point. A similar conclusion can be achieved for $p_3 = 0$ by using the Lyapunov candidate $V_{p_3} := \frac{1}{2}p_3^2$.

Remark 2: We refer to the control law (9)-(10) as quasi time-optimal to parallel with the definition given in [16] for the double integrator case. Note that when the gains k_\perp, k_3 are large, the closed-loop behavior approaches the one of the discontinuous time-optimal feedback $u := \begin{cases} -v_M \frac{p}{\|p\|} & \text{if } p \neq 0 \\ 0 & \text{if } p = 0 \end{cases}$

for single integrator saturated systems. Note that for any uniformly bounded $v_d(t)$, the proposed QTO law guarantees that the commanded follower velocity is bounded. \square

We conclude this section by stating the following corollary of Theorem 1, which is instrumental for the proof of our main result in the next section.

Corollary 1: Given the closed-loop system obtained by combining (8) and (9)-(10), for any positive selection of gains k_\perp , k_3 and saturation levels v_m , v_M , the set

$$\{p \in \mathbb{R}^3 : \|p_\perp\| \leq r, |p_3| \leq h\} \quad (12)$$

is contractively invariant for any scalars $r \in \mathbb{R}_{>0}$ and $h \in \mathbb{R}_{>0}$.

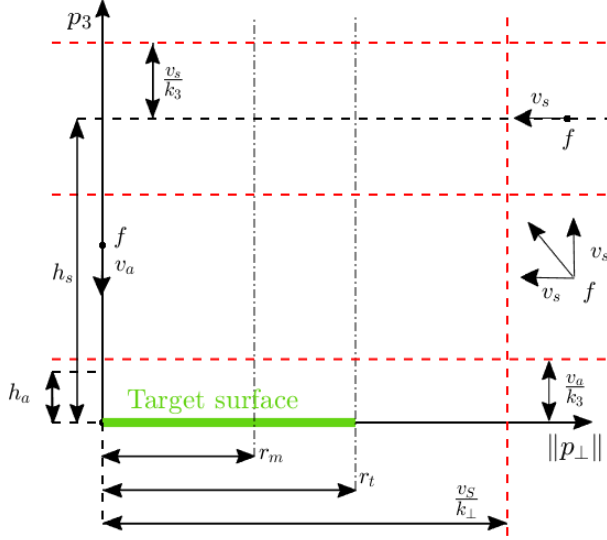


Figure 1. Main quantities involved in the hybrid logic and velocity of the follower (f) in different operating points.

B. Hybrid logic for safe landing

In this section we present a hybrid logic to solve Problem 1 based on the use of three operating modes. In mode 0 (synchronization), the follower is far from the target and has to get close to a safe relative position with respect to the target in a sufficiently fast way. In mode 1 (approach), the follower starts the approach maneuver which has to be performed in a sufficiently slow and controlled way. In mode 2 (land), the follower has reached a sufficiently close point above the target landing surface and therefore the landing command is activated.

The proposed strategy can be considered as a hybrid automaton, which we model using the framework of [17]. The different working modes outlined above are selected via a logical state $q \in Q := \{0, 1, 2\}$. For each mode the following domains, in which the state p evolves according to differential equations, are identified:

$$C_0 := \left\{ p \in \mathbb{R}^3 : \begin{cases} \|p_\perp\| \geq r_m & \text{if } p_3 \geq h_a \\ \|p_\perp\| \geq r_t & \text{if } 0 \leq p_3 < h_a \end{cases} \right\} \quad (13)$$

$$C_1 := \{p \in \mathbb{R}^3 : \|p_\perp\| \leq r_t, p_3 \geq h_a\} \quad (14)$$

$$C_2 := \{p \in \mathbb{R}^3 : \|p_\perp\| \leq r_t, p_3 = 0\} \quad (15)$$

where $h_a \in \mathbb{R}_{>0}$ defines the altitude at which the approach phase should end while $\mathbb{R}_{>0} \ni r_m < r_t$ is the radius at which the synchronization phase should end.

Remark 3: The choice $r_m < r_t$ will guarantee that switches between modes occur with hysteresis to avoid chattering phenomena. Sufficiently large values for $h_a > 0$ and $r_t - r_m > 0$ are also needed to give robustness to the proposed hybrid strategy which is developed on the basis of a kinematic model. Note, in passing, that sufficiently large values for $h_a > 0$ make the design robust to attitude variations of the target (Rem. 1). \square

We now introduce the main elements of the hybrid logic. The set of edges, identifying possible transitions between the modes, is given by $E := \{(0, 1), (1, 0), (0, 2), (2, 0), (1, 2), (2, 1), (2, 2)\}$. The guard conditions, giving for each edge the set $\text{Guard}(q, q')$ to which the error has to belong for transitions between q and q' to be possible, are:

$$\begin{aligned} \text{Guard}(0, 1) &:= \{p \in \mathbb{R}^3 : \|p_\perp\| \leq r_m, p_3 \geq h_a\}, \\ \text{Guard}(1, 0) &:= \{p \in \mathbb{R}^3 : \|p_\perp\| \geq r_t, p_3 \geq 0\}, \\ \text{Guard}(0, 2) &:= \{p \in \mathbb{R}^3 : \|p_\perp\| \leq r_t, 0 \leq p_3 \leq h_a\}, \\ \text{Guard}(2, 0) &= C_0, \quad \text{Guard}(1, 2) = \text{Guard}(0, 2), \\ \text{Guard}(2, 1) &= C_1, \quad \text{Guard}(2, 2) = \text{Guard}(0, 2). \end{aligned} \quad (16)$$

The reset map $\text{Reset} : E \times \mathbb{R}^3 \mapsto \mathbb{R}^3$, which describes for each edge (q, q') and state p the jump of the state p during a transition from q to q' , is given by:

$$\begin{aligned} \text{Reset}(0, 1, p) &= \text{Reset}(1, 0, p) = \text{Reset}(2, 0, p) \\ &= \text{Reset}(2, 1, p) := p + x_t, \quad \text{Reset}(0, 2, p) = \text{Reset}(1, 2, p) \\ &= \text{Reset}(2, 2, p) := [(p_\perp + x_{t_\perp})^\top \quad x_{t_3}]^\top. \end{aligned} \quad (17)$$

Note that through (17) we model the landing as a discontinuous phenomenon in which the follower is instantaneously brought to the target surface according to $\text{Reset}(\cdot, 2, p)$ when jumping conditions are met. In our experiment, the landing mode corresponds to the disarming of the follower³, which falls by gravity on the target surface. Hence, to account for this effect in the kinematic model, we assume that the input u acts also during jumps according to $p^+ = u - x_t^+ = u - x_t$.

At this point, to solve Problem 1, we suggest the following hybrid control law:

³In our specific application involving multirotor UAVs, the follower is disarmed, namely, turned off (f_c and τ_c are both set to zero in (2), (4)), to land so as to reduce the perturbations induced by the wakes of the follower propellers on the target propellers, which are mounted on the back of a knitted mesh surface to let propellers take in air and work properly.

$$u(p, q) := \begin{cases} \begin{bmatrix} -\text{sat}_{v_s}^+(p_\perp) + v_{t_\perp} \\ -\text{sat}_{v_s}^{v_s}(k_3(p_3 - h_s)) + v_{t_3} \end{bmatrix} & \text{if } q = 0, p \in C_0 \\ \begin{bmatrix} -\text{sat}_{v_s}^+(p_\perp) + v_{t_\perp} \\ -\text{sat}_{v_a}^{v_s}(k_3 p_3) + v_{t_3} \end{bmatrix} & \text{if } q = 1, p \in C_1 \\ v_t & \text{if } q = 2, p \in C_2 \\ \bigcup_{\{q': p \in \text{Guard}(0, q')\}} \text{Reset}(0, q', p) & \text{if } q = 0 \\ \bigcup_{\{q': p \in \text{Guard}(1, q')\}} \text{Reset}(1, q', p) & \text{if } q = 1 \\ \bigcup_{\{q': p \in \text{Guard}(2, q')\}} \text{Reset}(2, q', p) & \text{if } q = 2. \end{cases} \quad (18)$$

During the synchronization mode ($q = 0$) in the C_0 domain, the objective of the control law $u = [-\text{sat}_{v_s}^+(p_\perp)^\top \quad -\text{sat}_{v_s}^{v_s}(k_3(p_3 - h_s))]^\top$ is to track a point at a distance $\mathbb{R}_{>0} \ni h_s \gg h_a$ above the target point x_t , namely, $x_s := x_t + [0 \ 0 \ h_s]^\top$ which is henceforth called *safety approaching point* (see Figure 1). By properly selecting the saturation bounds v_s and the gains k_\perp, k_3 one can control the trajectory of the follower to ensure that the landing point is safely reached, *i.e.*, by keeping a sufficient distance from the target. To this regard, note that in saturated conditions the follower moves along straight lines (*e.g.*, making a 45deg angle with respect to the ground when using the same saturation levels for (9) and (10)). Instead, in the approaching mode ($q = 1$) in the C_1 domain, the objective of the control law is to track the target point x_t , with approaching vertical speed bounded by v_a . Then, in the absence of perturbations, the follower will enter the set $\text{Guard}(0, 2)$ in finite time and the reset condition $\text{Reset}(1, 2, p)$ will be activated so that $q^+ = 2$ and the follower will be brought to the target surface. Once there, the follower stays there for all future times, due to friction: we model this condition at the kinematic level according to the flow $\dot{p} = 0$ induced by u when $q = 2$ and $p \in C_2$.

Remark 4: The lower bound in $\text{sat}_{v_a}^{v_s}(k_3 p_3)$ of u_3 constrains the relative approaching speed of the follower to a given desired value v_a . In particular, the follower moves at the maximum allowable relative speed for any $\left\{ p \in \mathbb{R}^3 : p_3 \geq \frac{v_a}{k_3} \right\} \cap C_1$ during the approach mode. \lrcorner

Finally, by using $\dot{q} = 0$ to describe the dynamics of the logic variable during the flow, the system evolution can be studied by referring to a hybrid system in \mathbb{R}^4 , in which the state is given by $z := [q \ p^\top]^\top$:

$$\dot{z} = F(z) \quad z \in C, \quad z^+ \in G(z) \quad z \in D \quad (19)$$

where

$$C := (\{0\} \times C_0) \cup (\{1\} \times C_1) \cup (\{2\} \times C_2), \quad (20)$$

$$D := (\{0\} \times (\text{Guard}(0, 1) \cup \text{Guard}(0, 2))) \cup (\{1\} \times (\text{Guard}(1, 0) \cup \text{Guard}(1, 2))) \cup (\{2\} \times (\text{Guard}(2, 0) \cup \text{Guard}(2, 1) \cup \text{Guard}(2, 2))), \quad (21)$$

$$F(z) := \begin{cases} [-\text{sat}_{v_s}^+(p_\perp)^\top \quad -\text{sat}_{v_s}^{v_s}(k_3(p_3 - h_s))]^\top & \text{if } z_1 = 0 \\ [-\text{sat}_{v_s}^+(p_\perp)^\top \quad -\text{sat}_{v_s}^{v_a}(k_3 p_3)]^\top & \text{if } z_1 = 1 \\ [0 \ 0 \ 0]^\top & \text{if } z_1 = 2, \end{cases} \quad (22)$$

$$G(z) := \begin{cases} G_0 \left([z_2 \ z_3 \ z_4]^\top \right) & \text{if } z_1 = 0 \\ G_1 \left([z_2 \ z_3 \ z_4]^\top \right) & \text{if } z_1 = 1 \\ G_2 \left([z_2 \ z_3 \ z_4]^\top \right) & \text{if } z_1 = 2 \end{cases} \quad (23)$$

$$\text{with } G_q(y) := \bigcup_{\{q': y \in \text{Guard}(q, q')\}} [q' \ \text{Reset}(q, q', y)^\top]^\top, \quad y \in \mathbb{R}^3.$$

The next theorem relies on the properties of the proposed quasi time-optimal stabilizer and is our main result.

Theorem 2: Consider the hybrid dynamics (19) representing the closed-loop error dynamics obtained from (5) with control law (18) under Assumption 1 and 2. Then, for any choice $h_s > h_a$ and any selection of positive gains k_\perp, k_3 and saturation levels v_s, v_a , all the closed-loop solutions starting in the set $\Omega_0 := \{(q, p) \in Q \times \mathbb{R}^3 : p_3 \geq 0\}$ converge to the set $\Omega_\ell := \{(q, p) \in Q \times \mathbb{R}^3 : q = 2, \|p_\perp\| \leq r_t, p_3 = 0\}$ in finite time.

Sketch of the Proof. In the following we make use of the notation of [17] according to which a solution to systems of the form (19) is defined on a hybrid time domain $E \subset \mathbb{R}_{\geq 0} \times \mathbb{Z}_{\geq 0}$ where, for each $(t, j) \in E$, t measures the amount of elapsed ordinary time and j measures the number of jumps already performed by the solution. First of all, note that thanks to the properties of the QTO stabilizer established in Corollary 1 and the proposed hybrid logic, it can be shown that the set Ω_0 is forward invariant for (19). Consider the set $\Omega_1 := \{(q, p) \in Q \times \mathbb{R}^3 : \|p_\perp\| \leq r_t, p_3 = 0\} \cup Q \times \text{int}(\text{Guard}(0, 2))$. If $z(0, 0) \in \Omega_1$, proving the claim of the theorem is trivial, since either $z(0, 0) \in \Omega_\ell$ or the solutions from $z(0, 0) \in \Omega_1 \setminus \Omega_\ell$ just make a jump to Ω_ℓ , which is forward invariant for (19). To conclude the proof one can show that for any initial conditions in $\Omega_0 \setminus \Omega_1$ there exists a pair (t^*, j^*) such that $z(t^*, j^*) \in Q \times \text{Guard}(0, 2)$ and the solutions make a final jump to Ω_ℓ , *i.e.*, $z(t^*, j^* + 1) \in \Omega_\ell$. To this end note that $\Omega_0 \setminus \Omega_1$ can be split in a finite number of subdomains and, by exploiting the convergence properties of the QTO stabilizer, one can check the existence of (t^*, j^*) for any initial condition in the different subdomains. Due to space limitations, we omit this lengthy but straightforward part of the proof. \square

Remark 5: In case the follower exits for any reason the landing domain C_1 , the hybrid logic activates the synchronization mode and the follower is commanded to increase its relative altitude in order to get back to the safety point. To reduce the landing time, a slightly modified strategy, which we have implemented in the experiment, is to use h_s as an additional state of the logic which is updated by setting it equal to the relative vertical distance that has been achieved right before exiting the C_1 domain. \lrcorner

Finally, we would like to highlight that the region of convergence Ω_0 could be straightforwardly enlarged to include a large set also below the target surface ($p_3 < 0$) thanks the tracking properties of the QTO controller.

IV. EXPERIMENTAL RESULTS

A. Experimental setup

Flight tests are carried out inside the Flying Arena for Rotorcraft Technologies (FlyART) of Politecnico di Milano which is an indoor facility equipped with a Motion Capture system (Mo-Cap). The drone used as follower, codename ANT-R, is a quadcopter racer, while the target one, codename CARRIER-1, is an octocopter with a flat landing surface (Figure 2). Data are collected through the Mo-Cap system composed by 12 cameras which detect markers mounted on the drones. A ground control station receives measurements from the Mo-Cap system, reconstructs the relative state of the target with respect to the follower and then computes position and velocity set-points for the follower according to the hybrid logic presented in Section III-B. The QTO strategy has been integrated in the *PX4* autopilot [15] using *ANT-X* rapid prototyping system for multirotor control [18].



Figure 2. ANT-R and CARRIER-1 drones.

B. Flight test results

The landing has been performed with the target moving along a circular trajectory of radius $R = 1.5$ m and angular frequency $\omega = 0.5$ rad/s. Before the landing procedure is started, the follower is hovering around $[-3.5 \ 0 \ 2.8]^T$ m while the target is commanded to track a circular trajectory centered in $[-2 \ 0 \ 1.3]^T$ m with respect to the inertial frame of the flying arena. The automatic landing procedure is activated two seconds after the target has started tracking the circular trajectory. A video of the experiment is available online⁴.

Figure 3 shows the position of the two drones during the experiment together with the target desired trajectory. In the figure, circle, cross and star markers are used to identify the switchings of the logic variable q : in correspondence of circle markers $q = 0$ and the synchronization mode is activated, in correspondence of cross markers $q = 1$ and the approach phase begins while in correspondence of star markers, $q = 2$ and the disarm command is sent to the follower. The behavior of the proposed control strategy is clearer when referring to Figure 4 and Figure 5, in which the in-plane position trajectories of

the two drones and the vertical error are reported, respectively. The evolution of the logic variable is plotted together with the vertical error in Figure 5. As can be observed, at the beginning of the landing procedure the follower is far from the target with the logic variable initialized at 0. In this condition, the synchronization mode is active and the follower tracks the safety point above the follower at a relative vertical distance $h_s = 1.5$ m, namely, $x_s = x_t + [0 \ 0 \ 1.5]^T$ m. When the in-plane error p_{\perp} is less than $0.15 = r_m < r_t = 0.25$ m, the logic variable switches to 1, the saturation level on the vertical velocity controller is changed to the lower value $v_a = 0.3$ m/s and the follower starts the approach phase. Note that the large initial error makes the follower exit the C_1 region right after entering it and therefore the logic state is switched back to synchronization mode again. Hence, the follower tries to get back to an updated safety point above the target having the same relative vertical altitude reached before exiting the landing domain (Remark 5). When the in-plane distance is again lower than r_m , q jumps to 1. At this point the controller is able to keep the follower in the C_1 domain until the land mode is activated. In Figure 5 one can see that while the follower is out of the landing region ($q = 0$) and before any jump to the approach mode has occurred, the vertical position set-point of the follower is the safety point at 1.5 m above the target while after the first switch, the new safety point is located above the target at the previously achieved vertical distance. The landing procedure ends when p_3 is below the approach altitude h_a , which is represented by the black dashed line in Figure 5. When this condition is verified, q jumps to 2, and the follower is disarmed. Finally, by inspecting Figure 6, it can be verified that during most of the approach phase the magnitude of the follower vertical velocity is almost coincident with the value of the saturation level v_a since the target vertical velocity is almost null. When the follower is near the target with $p_3 < \frac{v_a}{k_3}$, the QTO controller works in the unsaturated regime and the relative velocity is linearly reduced, thereby making the touchdown smoother.

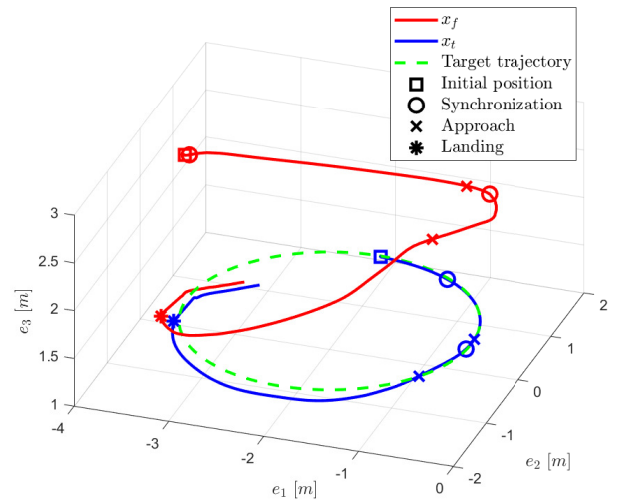


Figure 3. Position of follower and target from the beginning of the target trajectory to 3 seconds after landing.

⁴Visit <https://youtu.be/r6GhIOcf--0> or the ASCL group website <http://ascl.daer.polimi.it>.

V. CONCLUSIONS

In this paper we tackled the problem of AAAL of UAVs for the solution of which a hybrid logic combined with a QTO tracking controller has been developed. By referring to a kinematic model of the UAV, our strategy enables automatic landing of a UAV on the landing surface of a carrier drone in a safe and quasi time-optimal way. An experimental campaign involving two multirotor UAVs has shown the effectiveness of the proposed strategy.

REFERENCES

- [1] T. Paul, T. R. Krogstad, and J. T. Gravdahl, "Modelling of UAV formation flight using 3D potential field," *Simulation Modelling Practice and Theory*, vol. 16, no. 9, pp. 1453–1462, 2008.
- [2] F. Borrelli, T. Keviczky, and G. J. Balas, "Collision-free UAV formation flight using decentralized optimization and invariant sets," in *2004 43rd IEEE Conference on Decision and Control*, vol. 1, Dec 2004, pp. 1099–1104 Vol.1.
- [3] J. Valasek, K. Gunnam, J. Kimmet, M. D. Tandale, J. L. Junkins, and D. Hughes, "Vision-based sensor and navigation system for autonomous air refueling," *Journal of Guidance, Control, and Dynamics*, vol. 28, no. 5, pp. 979–989, 2005.
- [4] B. Hu, L. Lu, and S. Mishra, "A control architecture for time-optimal landing of a quadrotor onto a moving platform," *Asian Journal of Control*, vol. 20, no. 5, pp. 1701–1712, 2018.
- [5] B. Herisse, T. Hamel, R. Mahony, and F.-X. Russotto, "Landing a VTOL unmanned aerial vehicle on a moving platform using optical flow," *IEEE Transactions on Robotics*, vol. 28, pp. 1 – 13, 2012.
- [6] D. Lee, T. Ryan, and H. J. Kim, "Autonomous landing of a VTOL UAV on a moving platform using image-based visual servoing," in *IEEE International Conference on Robotics and Automation, Saint Paul, USA*, 2012.
- [7] A. Borowczyk, D.-T. Nguyen, A. Phu-Van Nguyen, D. Q. Nguyen, D. Saussié, and J. Le Ny, "Autonomous landing of a multirotor micro air vehicle on a high velocity ground vehicle," *IFAC-PapersOnLine*, vol. 50, no. 1, pp. 10488–10494, 2017.
- [8] P. Giuri, A. Marini Cossetti, M. Giurato, D. Invernizzi, and M. Lovera, "Air-to-air automatic landing for multirotor UAVs," in *5th CEAS Conference on guidance, navigation and control (EuroGNC)*, Milan, Italy, April 2019.
- [9] Giurato, M., "Design, integration and control of multirotor UAV platforms." Ph.D. dissertation, Politecnico di Milano, 2019.
- [10] M. Giurato, P. Gattazzo, and M. Lovera, "UAV Lab: a multidisciplinary UAV design course," *IFAC-PapersOnLine*, vol. 52, no. 12, pp. 490–495, 2019.
- [11] M.-D. Hua, T. Hamel, P. Morin, and C. Samson, "Introduction to feedback control of underactuated VTOL vehicles: A review of basic control design ideas and principles," *IEEE Control Systems*, vol. 33, no. 1, pp. 61–75, 2013.
- [12] D. Invernizzi, M. Lovera, and L. Zaccarian, "Geometric trajectory tracking with attitude planner for vectored-thrust VTOL UAVs," in *2018 Annual American Control Conference (ACC)*, 2018, pp. 3609–3614.
- [13] —, "Integral ISS-based cascade stabilization for vectored-thrust UAVs," *IEEE Control Systems Letters*, vol. 4, no. 1, pp. 43–48, Jan. 2020.
- [14] —, "Dynamic attitude planning for trajectory tracking in thrust-vectoring UAVs," *IEEE Transactions on Automatic Control*, vol. 65, no. 1, pp. 453–460, 2020.
- [15] PX4-Community, "Documentation available at <https://docs.px4.io/en/>," Tech. Rep., 2018.
- [16] F. Forni, S. Galeani, and L. Zaccarian, "A family of global stabilizers for quasi-optimal control of planar linear saturated systems," *IEEE Transactions on Automatic Control*, vol. 55, no. 5, pp. 1175–1180, May 2010.
- [17] R. Goebel, R. G. Sanfelice, and A. R. Teel, *Hybrid Dynamical Systems*. University Press Group Ltd, 2012.
- [18] ANT-X website, <https://antx.it/>.

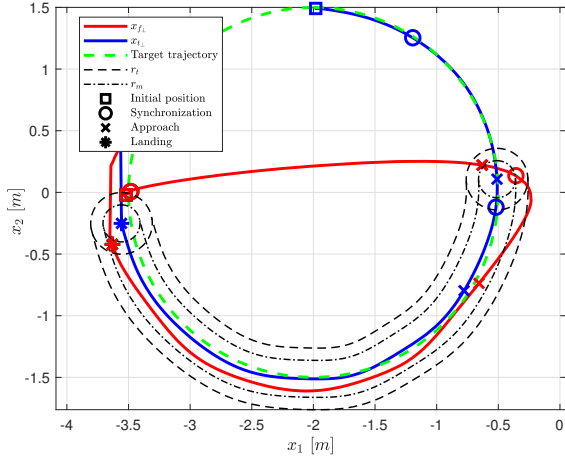


Figure 4. In-plane position of follower and target from the beginning of the target trajectory to 3 seconds after landing.

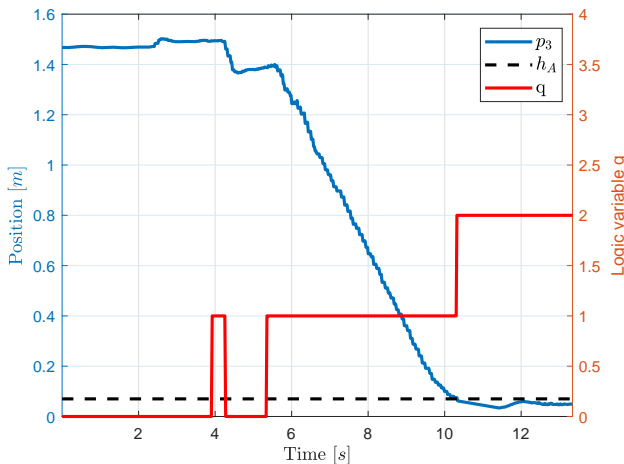


Figure 5. Vertical position time history from the beginning of the target trajectory to 3 seconds after landing.

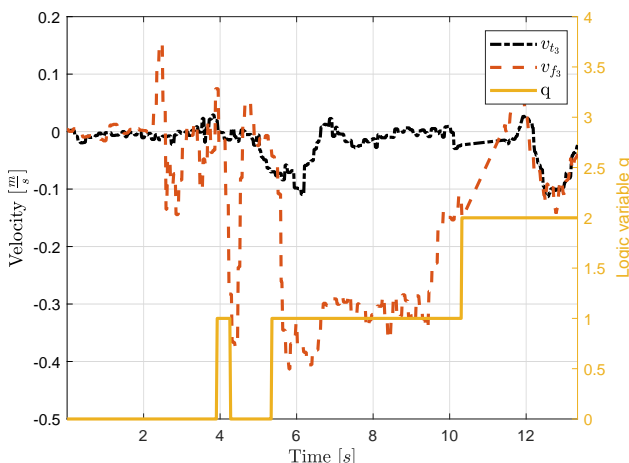


Figure 6. Vertical velocity time history from the beginning of the target trajectory to 3 seconds after landing.